COMMUNICATIONS IN SCIENCE AND TECHNOLOGY
Homepage: cst.kipmi.or.id

Efficient removal of amoxicillin, ciprofloxacin, and tetracycline from aqueous solution by Cu-Bi_2O_3 synthesized using precipitation-assisted-microwave

Fatkhiyatus Sa'adah[a,d], Heri Sutanto[b,d,*], Hadiyanto Hadiyanto[c], Ilham Alkian[a,d]

[a]*Doctoral Program of Environmental Science, Diponegoro University, Semarang 50275, Indonesia*
[b]*Department of Physics, Diponegoro University, Semarang 50275, Indonesia*
[c]*Department of Chemical Engineering, Diponegoro University, Semarang 50275, Indonesia*
[d]*Smart Material Research Center, Diponegoro University, Semarang 50275, Indonesia*

Article history:
Received: 28 May 2024 / Received in revised form: 21 June 2024 / Accepted: 23 June 2024

Abstract

This study investigates the synthesis and characterization of Cu-Bi_2O_3 for degradation of antibiotics AMX, CIP, and TC using precipitation-assisted-microwave method at varying concentrations of Cu at 0%, 2%, 4%, 6%, and 8%. The effect of Cu concentration on the structural, morphological, and optical properties were studied by XRD, UV-Vis, and SEM-EDX. The optimal results were obtained by adding 4% Cu to the Bi_2O_3 matrix. With an energy band gap of 2.32 eV, a crystal size of 37.04 nm, and α-Bi_2O_3 and $CuBi_2O_4$ phases. The removal efficiency of each antibiotic using the photocatalytic method varies, with AMX at 52.06%, CIP at 61.72%, and TC at 69.44%. Cu-Bi_2O_3 degraded TC-type antibiotics more rapidly. The high removal efficiency and rapid reaction rate indicate that Cu-Bi_2O_3 is an effective antibiotic removal agent. This further confirms the fact that the addition of Cu to Bi_2O_3 material can increase its ability to degrade antibiotics more effective.

Keywords: Bismuth oxide; antibiotics; photocatalyst; Cu; degradation

1. Introduction

Antibiotics are emerging pollutants or novel pollutant compounds that have not yet been regulated [1]. Antibiotics of various classes have been found in hospital effluent [2], residential wastewater [3], slurry [4], water to consume [5], groundwater [6], air surface water [7], sediment [8] and land [9]. It's important to remember that the biotechnology approach that is commonly used by wastewater treatment plants hasn't been shown to break down antibiotics yet. Instead, it just moves pollutants from one phase to another and helps microbes become resistant to antibiotics that get stuck in physical filters [2].

The entry of antibiotics into the ecosystem can damage the environment. Antibiotic residues will be in the environment for a long time because antibiotics are not readily biodegradable [10]. Therefore, an effective and efficient method is needed to overcome the problem of antibiotic pollution. Several techniques for degrading antibiotics have been reported, but the effectiveness of removing antibiotics remains relatively low [11]. Photodegradation [12–14], Fenton-like processes [15], adsorption methods [16], coagulation [17], membrane separation [18], and aerobic and anaerobic degradation [19] are some ways that antibiotics have been removed. Researchers are using the Advance Oxidation Process (AOP) method to create an antibiotic degradation technique [20–24]. Because of their eco-friendly, green-process methods and low cost, AOPs have been extensively used as a technology in the degradation process, making them more productive and effective in offering antibiotic pollution solutions. Using an oxidation reaction process, the AOP involves the generation of sufficient hydroxyl radicals (·OH) and superoxide radicals (O_2^{-}·) to purify waste. The photocatalytic method has promising applications since it can to carry out oxidation reactions, produce hydroxyl radicals, and is both sustainable and environmentally friendly [25].

Bismuth oxide (Bi_2O_3) is a common photocatalyst that exhibits outstanding photocatalytic performance in water separation, organic waste treatment, and antibiotic pollution treatment. Because Bi_2O_3 has a bandgap spanning from 2.1 to 2.8 eV, it is more effective for visible light absorption. The crystalline phase structure of Bi_2O_3 greatly influences its characteristics [26]. The photocatalytic activity of Bi_2O_3 is extremely dependent on its crystalline structure and morphology. Although it has been established that Bi_2O_3 has good photocatalytic performance and efficiently utilizes visible

* Corresponding author.
Email: herisutanto@live.undip.ac.id
https://doi.org/10.21924/cst.9.1.2024.1444

light, some parameters, such as stability and solubility, should be highlighted [27].

Recently, several reports have been published on the recent progress of Bi_2O_3 and their application. Unfortunately, few literatures have systematically summarized the synthesis techniques of Bi_2O_3 and their application in the antibiotic degradation, which is a big challenge [28]. Bi_2O_3 photocatalyst quality is significantly influenced by the Bi_2O_3 synthesis method. Metal doping is one of the most efficient methods for enhancing the photocatalytic activity of Bi_2O_3 materials [29].

Dopants of metals such as Fe [30], Ni [31], Zn [32], and Ce [33] in Bi_2O_3 may interact to enhance photocatalytic performance, according to some research. Due to its widespread use in metal-doped semiconductor photocatalysts, cuprum (Cu) is a possible dopant metal. In addition, the smaller size of Cu atoms compared to Bi makes it simpler to replace ions to enhance photocatalytic activity [34].

In this paper, Cu-Bi_2O_3 was synthesized through homogeneous precipitation-assisted-microwave. The effect of Cu dopant concentration in the Bi_2O_3 matrix as material for antibiotic removal will be investigated and compared to its photocatalytic activity. In addition, we demonstrated that Cu-Bi_2O_3 is an effective removal agent for amoxicillin (AMX), ciprofloxacin (CIP), and tetracycline (TC)-type antibiotics under UV-Light irradiation. Various removal methods, such as adsorption, photolysis, and photocatalysis, will determine the effect of using Cu-Bi_2O_3 catalyst material in removing of antibiotics compare without doping materials. To the best our knowledge, this method can show the most efficient and inexpensive way to remove antibiotics on a large scale. To analyze the band gap energy, structure, and morphology of Cu-Bi_2O_3, ultraviolet-visible (UV-Vis) X-ray Diffraction (XRD) and scanning electron microscopy (SEM) analyses were performed. Several methods of antibiotic degradation, such as adsorption, photolysis, and photocatalysis, are utilized to determine the kinetic parameters of the antibiotic removal processes.

2. Materials and Method

2.1. Materials

Bismuth nitrate pentahydrate Bi $(NO_3)_3.5H_2O$ (Sigma-Aldrich Ltd, 98%) as Bi precursor. Copper (II) Nitrate Cu $(NO_3)_3.3H_2O$ (Sigma-Aldrich Ltd, 98%) as Cu precursor. Natrium hydroxide NaOH (Merck, 1 mol/L) was precipitant. Nitric acid HNO_3 (Merck KgaA, 5%) and demineralized water (DW) were utilized as solvents.

Table 1. Physical and chemical properties of AMX, CIP, and TC

Antibiotic	Molecular weights ($g.mol^{-1}$)	Molecular formula	Density ($g.ml^{-1}$)	Type
Amoxicillin [35]	419.4	$C_{16}H_{19}N_3O_5S$	0.8	β-lactam
Ciprofloxacin [36]	331.4	$C_{17}H_{18}FN_3O_3$	1.5	Quinolone
Tetracycline [37]	444.4	$C_{22}H_{24}N_2O_8$	1.7	Tetracycline

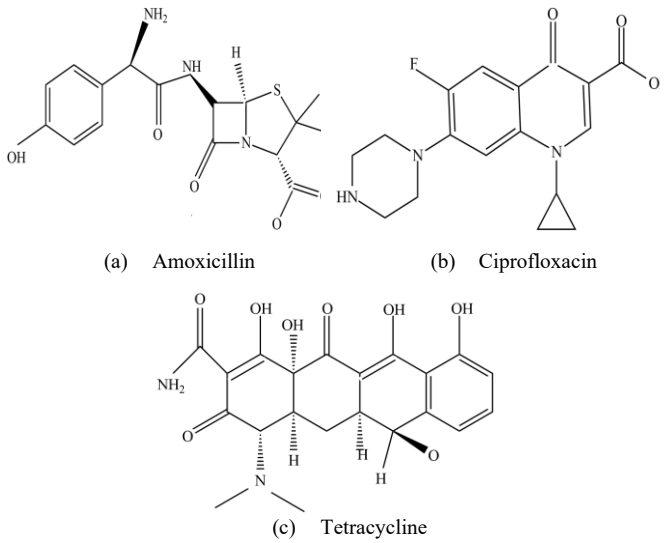

Fig. 1. Chemical structure of amoxicillin, ciprofloxacin, and tetracycline

Three antibiotics such as amoxicillin, ciprofloxacin, and tetracycline were obtained from a pharmaceutical company in Indonesia as a source of antibiotics. Their chemical structures are shown in Fig. 1 and some physical and chemical properties are listed in Table 1.

2.2. Synthesis of Cu-Bi_2O_3

Cu-Bi_2O_3 was synthesized using the precipitation-assisted microwave method by following previously described research [26]. 1 gram of bismuth nitrate was dissolved in 100 mL of nitric acid 5% and stirred using a magnetic stirrer on a hotplate for 10 minutes. Then, copper nitrate with a concentration variation of 0%, 2%, 4%, 6%, and 8% was stirred for 10 minutes until evenly mixed. After that, 500 mL of sodium hydroxide is added to the solution and stirred for 2 hours to produce a suspension. Then separate the precipitate and dry it to produce the powder. The powder was then fed into a microwave reactor. After the heating process, Cu-Bi_2O_3 powder will be produced.

The process of the synthesis of Cu-Bi_2O_3 is completely visible in Fig. 2.

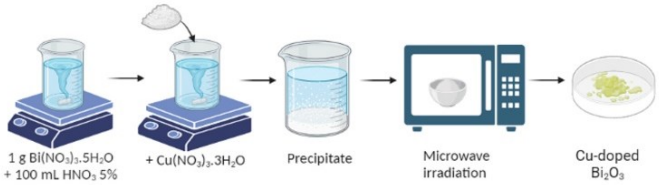

Fig. 2. The synthesis procedure of Cu-Bi_2O_3 material.

2.3. Characterization of Cu-Bi_2O_3 material

The optical properties of Cu-Bi_2O_3 were performed from the characterization results using a UV-Vis spectrophotometer (UV-Vis 1240 Shimadzu). The optical parameters analyzed in this study are energy band gap values, one of the important indicators that can be used to explain the photocatalytic ability. The energy band gap was determined by transmittance value data and analyzed using the Tauc plot method. The morphology

and elements of Cu-Bi_2O_3 were characterized using Scanning Electron Microscopy- Energy Dispersive X-ray (SEM JEOL JSM 6360). Crystal structure analysis was obtained using an X-ray Diffractometer (PANanalytical, XRD Shimadzu 6100/7000 type). The average crystal size of Cu-Bi_2O_3 was calculated using the Debye-Scherrer formula:

$$D = \frac{0.9\lambda}{\beta cos\theta} \quad (1)$$

where D represents crystallite size, λ is the wavelength of X-ray, β denotes Full Width and Half Maximum (FWHM) value, and θ is the diffraction angle.

2.4. Antibiotic degradation experiment under UV-light

Experiments on antibiotic removal were analyzed using adsorption, photolysis, and photocatalysis techniques. All experiments were performed in box equipped by UV-C lamps. The adsorption of antibiotic was carried out using batch method in the dark without UV light. The photolysis of antibiotic was first evaluated in the absence of Cu-Bi_2O_3 material under UV light irradiation. The photocatalysis process is using Cu-Bi_2O_3 material and irradiating with UV-C lamp.

Experiments were conducted using an antibiotic solution with a concentration of 1,000 mg. L-1. In 100 mL of AMX, CIP, and TC antibiotic solutions, 10 mg of Cu-Bi_2O_3 material was added to the samples. The mixture was stirred with a magnetic stirrer at a speed of 500 rpm and a temperature of 303 K at room temperature. Samples were collected for removal experiments involving adsorption, photolysis, and photocatalysis, which lasted 180 minutes. The samples were collected every 30 minutes and centrifuged at 10000 rpm for 5 minutes. UV light is utilized in the process of irradiating light. To determine the effect of using a Cu-Bi_2O_3 catalyst material in the removal of antibiotics, multiple methodologies will be employed. The processed antibiotic samples were then analyzed with a UV-Vis spectrophotometer for residue.

The UV-Vis spectrophotometer (UV-Vis 1240 Shimadzu) was used along with its corresponding absorption spectra before and after treatment to assess the concentration of the AMX, CIP, and TC solution. The photometry method utilized in this study is derived from Riyanti et.al.[38]. The removal efficiency for each process (adsorption, photolysis, and photocatalysis) was calculated using equation 2:

$$RE(\%) = \frac{(C_o - C_t)}{C_o} x100 \quad (2)$$

where RE (%) is removal efficiency, C_o (mg. L^{-1}) represents the initial concentration, C_t (mg. L^{-1}) represents the concentration of antibiotic at contact time (t).

The Langmuir-Hinshelwood equation is a common way to characterize the reaction kinetics of photocatalytic degradation. The Langmuir-Hinshelwood equation is expressed as follows:

$$\frac{1}{r} = \frac{1}{k_r} + \frac{1}{k_r k_a C} \quad (3)$$

If the reaction takes place at extremely low concentrations (mg. L^{-1}), and the reaction proceeds as a first-order reaction so that

$$\frac{1}{r} = \frac{1}{k_r}; r = k_r \quad (4)$$

$$r = \frac{d[C]}{dt} = -k[C]^1 \quad (5)$$

$$r = \frac{d[C]}{[C]} = -k\, dt \quad (6)$$

with the r is initial rate (mol.L^{-1}.min^{-1}), k is reaction rate constant (mol.L^{-1}.min^{-1}), and k_r is adsorption coefficient.

If the concentration at time t = 0 is [C_o] and at contact time t = t is [C_t], then the rate law of the reaction can be obtained through the integral on the limit 0 to t:

$$\int_{[C_o]}^{[C]} \frac{d[C]}{[C]} = -k_r \int_0^t dt \quad (7)$$

$$r = \frac{ln\,[C]}{[C_o]} = -k_r t \quad (8)$$

The reaction rate is directly proportional to the reaction rate setting, which the setting's magnitude can determine. The reaction rate is determined by plotting the function ln [C]/[C_o] against time, where C is the concentration of the antibiotic after degradation for a certain amount of time and Co is the initial concentration of the antibiotic [39].

3. Results and Discussion

3.1. Characteristics of Cu-Bi_2O_3

The synthesized Cu-Bi_2O_3 has an energy band gap level of 2.32 – 2.86 eV, presented in Fig. 3. This result is consistent with previous research regarding the energy band gap region of Bi_2O_3. The band gap energy of Bi_2O_3 is less than 3.0 eV [40]. Based on these data, the lowest energy band gap value of 2.32 eV was obtained by adding 4% Cu. As the Cu concentration in the Bi_2O_3 matrix increases, the band gap energy decreases until it reaches 4%. The energy band gap increased by 2.84 eV when the concentration was raised to 6%. By raising the concentration of Cu dopant by more than 4%, the absorbance will decrease, resulting in a wider optical energy band gap. The energy band gap of the 6% Cu sample exhibits an increase, which can be attributed to a reduction in surface roughness. When the concentration of Cu exceeds 4% to 6%, the structure of Bi_2O_3 begins to disappear. It is possible that Cu plays a role in the optical characteristics, and attributed to the increase in grain size with the increase in copper concentration [41].

These results demonstrate that the addition of Cu to the proper Bi_2O_3 matrix is proven to be able to reduce the energy band gap. The reduction in the energy band gap of Cu-Bi_2O_3 can be attributed to the enlargement of the grain size [42]. The resulting band gap energy value shows that Bi_2O_3 has good performance under visible light. The smaller energy band gap is produced, the less space is required between the valence band and the conduction band, facilitating the photocatalytic production of electrons and holes. Consequently, photocatalytic activity is increased [30]. This analysis concluded that Cu-Bi_2O_3 4% was the most successfully synthesized material. These results will be confirmed through the consequences of XRD and SEM-EDX characterization.

The structure of Cu-Bi_2O_3 was analyzed using XRD, with the results illustrated in Fig. 4. In Fig. 4, the diffraction peaks were shown at 2θ = 12.75^0; 24.55^0; 25.82^0; 27.46^0; 30.04^0; 33.16^0; 35.24^0; 37.72^0; 42.28^0; 46.54^0; 48.65^0; 51.92^0; 56.84^0

and 62.8^0. These peaks corresponded to the miller index (011), (111), (002), (120), (012), (121), (210), (112), (032), (221), (104), (212), (320) and (321). Cu-Bi_2O_3 had the structure of α-Bi_2O_3 and Copper Bismuth Oxide ($CuBi_2O_3$). The resulting diffraction peaks correspond with pdf data card number ICDD-00-001-0709 and ICDD-00-026-0502. The average crystal size was 37.04 nm, obtained using the Debye-Scherer formula (Equation 1). The phase percentage of α-Bi_2O_3 and $CuBi_2O_4$ were respectively 77.8% and 22.2%. It indicates that the Cu-Bi_2O_3 4% has a primary phase of α-Bi_2O_3 and a secondary phase of $CuBi_2O_4$. The diffraction pattern of α-Bi_2O_3 correspond to the monoclinic structure with lattice parameters a: 5.83°, b: 8.14°, c: 7.48°, and α: γ: 90°, and β: 67.07° with space group p21/c and volume cell 326.92 m^3. It was known that monoclinic α-Bi_2O_3 is a stable phase allotrope at room temperature.

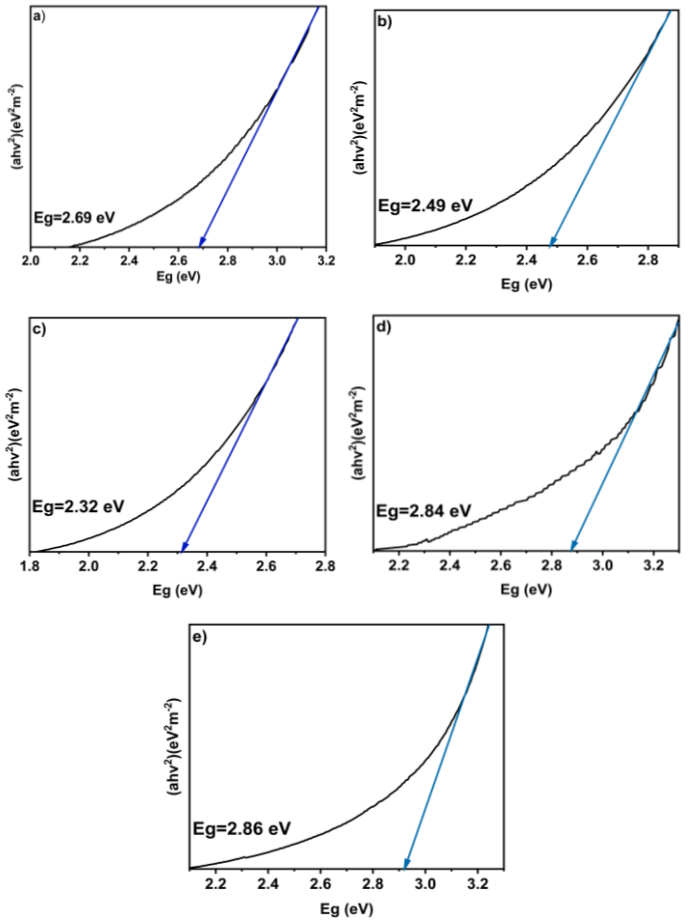

Fig. 3. The energy band gap of Cu-Bi_2O_3 (a) 0%, (b) 2%, (c) 4%, (d) 6%, and (e) 8%

Alternatively, the newly observed peaks were identified as belonging to the tetragonal $CuBi_2O_4$ crystal structure, characterized by lattice parameters a: b: 8.51°, and c: 5.814°, and α: β: γ: 90°. The crystal structure belongs to the p4/ncc space group and has a cell volume of 421.05 m^3. CuBi2O4 was synthesized using the solid-state interaction of Bi_2O_3 and CuO, with a low concentration of additional dopant. This indicates the high reactivity of the resulting materials, as documented in the literature [43]. The formation of the secondary phase occurs when a significant concentration of Cu dopant is added to Bi_2O_3, leading to an interaction between Bi and Cu atoms. This reaction results in partial replacement of Bi atoms by Cu atoms. Specific Cu dopants can enhance the degree of crystallinity. The α-Bi_2O_3 is a stable phase and has a monoclinic crystal structure. The high and sharp diffraction peaks designated Cu-Bi_2O_3 had a good crystallinity. It is also believed that crystallinity is a crucial parameter that influences the efficacy of photocatalysts. α-Bi_2O_3 has good crystallinity, so it plays a role as a recombination center, and it exhibits negligible reactivity in several photocatalytic reactions [44].

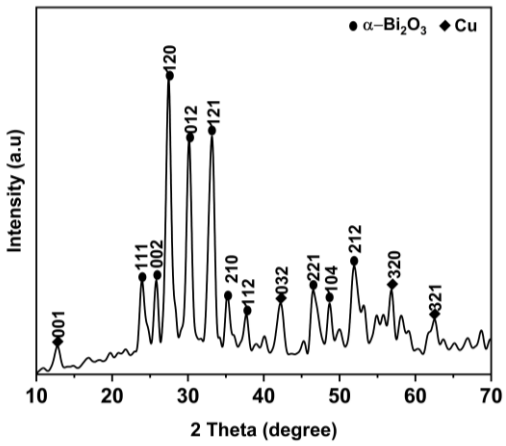

Fig. 4. The XRD Pattern of Cu-Bi_2O_3 4%

Morphological investigations were executed with the help of Scanning Electron Microscope (SEM) analysis presented in Fig. 5(a). The results show that the Cu-Bi_2O_3 samples consist of rod structure and spherical shapes like plate. The rod structure indicated the structure of Bi_2O_3 which is consistent with the previous research [45]. Plate-like structures indicated the Cu structure, and can offer a larger surface area, potentially leading to enhanced photocatalytic activity. In addition, the presence of amorphous materials was found, representing the doping material (Copper) and effectively connected the surface of Bi_2O_3. These results are consistent with the research before [46,47].

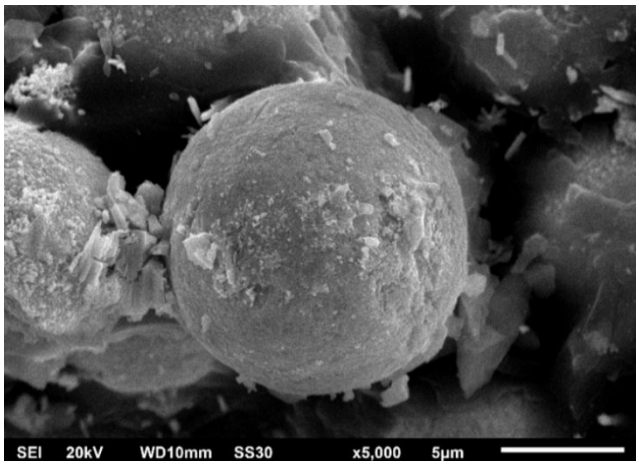

Fig. 5. The SEM image of Cu-Bi_2O_3 4%

Energy Dispersive X-ray (EDX) analysis was performed to identify the elemental constitution of the Cu-Bi_2O_3 synthesized materials. The spectrum analysis validated the purity of the prepared samples, as depicted in Fig. 6, providing evidence for the successful synthesis of Cu-Bi_2O_3 by verifying the existence of Cu, Bi, and O elements in the material's structure. The sample did not exhibit any peaks other than those

corresponding to Cu ions, indicating that the produced material is pure. Deliberately adding these metallic components is recognized to enhance the photocatalytic activity of Bi_2O_3 compositions. The presence of copper in Bi_2O_3 materials enhances their photodegradation activity, leading to a synergistic effect that improves the effectiveness of antibiotics. The distribution of the doped elements within the materials' structure is a critical determinant of their photodegradation capacity. The doped materials have the ability to release copper ions when they come into contact with antibiotics. These copper ions operate as a reducing agent and further decrease the concentration of the antibiotic solution.

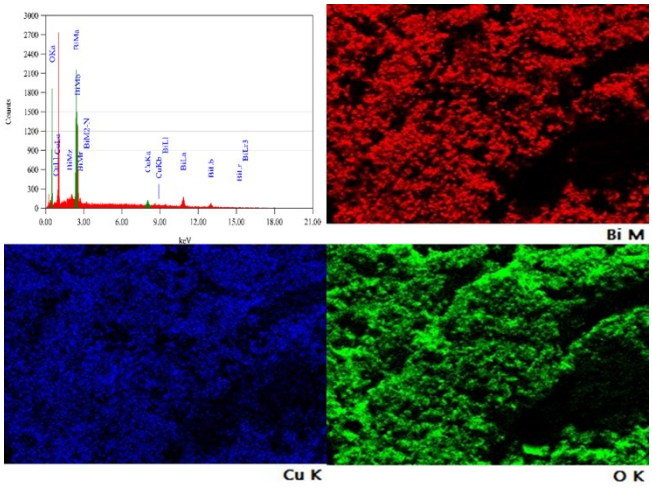

Fig. 6. EDX image and element mapping

3.2. Effect of Cu dopant for AMX, CIP, and TC degradation

The great change in the morphology, composition, and band structures inevitably impacts the photocatalytic activity of Cu-Bi_2O_3. The results of the adsorption, photolysis, and photocatalysis tests are presented in Fig. 7. The degradation processes of AMX, CIP, and TC are significantly affected by the Cu concentrations in Bi_2O_3. The photocatalysis method using 4% Cu-Bi_2O_3 showed a maximum elimination of 52.06% AMX, and a maximum CIP removal of 61.72%. Additionally, utilizing Cu-Bi_2O_3 at 4% in the photocatalysis approach, a maximum of 69.46% TC elimination was noted.

The presence of Cu^{2+} ions in Cu-Bi_2O_3 enhances its photocatalytic activity compared to pure Bi_2O_3, as a result of the synergistic interaction between Cu^{2+} ions and Bi_2O_3. The Bi_2O_3 doped with 4% Cu has the highest degrading efficiency. The results suggest that the addition of Cu in Bi_2O_3 up to a maximum concentration of 4% enhances the photocatalytic activity. However, beyond this concentration limit leads to a decline in the photocatalytic activity. These results align with the energy band gap of materials. The photocatalytic activity of a material can be correlated with its energy band gap. The smallest energy band gap is observed at a doping concentration of 4% Cu in Bi_2O_3, as determined by the photocatalytic activity test.

Additionally, the highest efficiency and optimal rate are also achieved at the same 4% Cu doping level. A smaller energy band gap indicates a higher photocatalytic capacity [48]. Furthermore, the photocatalytic activity is influenced by the presence of Cu particles that exhibit a porous spherical morphology on the surface of the Bi_2O_3 semiconductors, as depicted in the SEM image. The presence of a porous surface can enhance the surface area of the photocatalyst materials, while the inclusion of Cu transition metal can inhibit the rate at which electron-hole recombination occurs, hence increasing the photocatalytic activity.

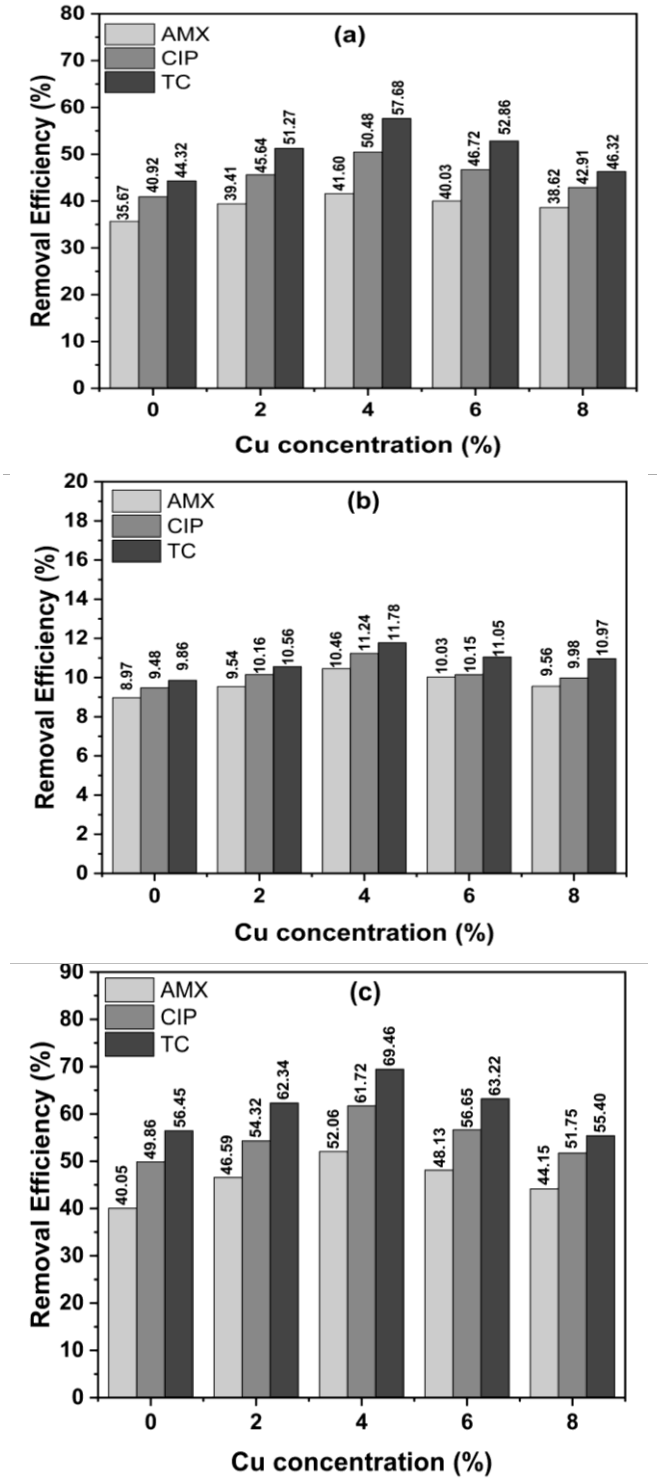

Fig. 7. Experimental conditions and their outcomes (a) Adsorption, (b) Photolysis, and (c) Photocatalysis

3.3. Removal of AMX, CIP and TC

As an agent for antibiotic breakdown, photocatalyst material is one of its uses. AMX, TC, and CIP were some antibiotics

employed in this investigation. The chosen material, 4% Cu-Bi_2O_3, is the best created throughout the synthesis step. Three methods degrade antibiotics used in this research: adsorption, photolysis, and photocatalysis. Each of the three procedures required 180 minutes of irradiation.

Adsorption is a method for adsorbing pollutants using a substance known as an adsorbent [49]. In this method of adsorption, Cu-Bi_2O_3 was used as an antibiotic adsorbent. Antibiotic solution was added by Cu-Bi_2O_3 and placed into box allowed to stand for 180 minutes for the achievement of an adsorption equilibrium. Each variety of antibiotics has a unique removal efficiency value. The removal efficiency of TC-type antibiotics was the highest (57.68%), followed by CIP (50.48%) and AMX (41.6%). Fig. 8 demonstrates that a greater than 50% TC removal efficiency was attained in the first 30 minutes of contact time. During the first 30 minutes of contact, CIP has an elimination efficiency of approximately 40% and AMX approximately 30%. After 30 minutes of contact time, the removal efficiency value did not substantially increase until 180 minutes of contact time. 30 minutes is the time for the achievement of an adsorption equilibrium so that after 30 minutes the adsorption process does not occur significantly. After 30 minutes of contact, the adsorption rate stabilized without significantly increasing. Because the concentration decrease is not continuous, these results indicate that the adsorption method for antibiotic degradation is ineffective. This is because the adsorbed ions can undergo further desorption if the adsorbent is not handled further, causing the adsorbent to reach saturation and preventing the adsorption process from being carried out [50].

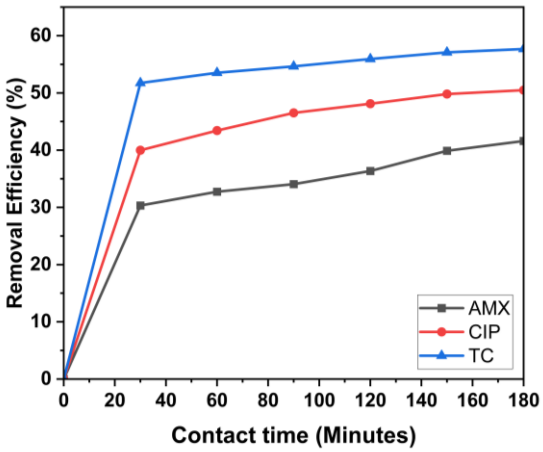

Fig. 8. Removal efficiency at contact time using adsorption method

The adsorption of antibiotics on Cu-Bi_2O_3 is a complex process comprising several steps, including the transfer of antibiotics from an aqueous solution into Cu-Bi_2O_3, diffusion on both the interior and external surfaces, and ultimately immobilization on the Cu-Bi_2O_3. There are several types of interactions that can be linked to the adsorption process, such as charge-dipole, hydrophobic, π-π, and electrostatic interactions [51]. The presence of functional groups such as -COOH, -NO_2, and -OH in antibiotic molecules allows them to establish hydrogen bonds with the surface of the sorbent, which is Cu-Bi_2O_3. Selecting the suitable material features to serve as a sorbent is crucial for facilitating the antibiotic breakdown process effectively.

Photolysis is one method for degrading compounds using only specific wavelengths of light. The process will chemically produce hydroxyl radicals (·OH) in the solution. These radical species are generated by the hole degeneration (h^+) process, which then reacts with water molecules. Hydroxyl radicals will attack organic compounds to initiate the mineralization process [52]. In this investigation, ultraviolet light was used to degrade antibiotics via photolysis (UV-C lamp).

As depicted in Fig. 9, the process of antibiotic degradation by photolysis is considered less effective due to the small decrease in concentration. This can be caused by the few oxidizing species formed due to photon induction, so the ability of antibiotic compounds to break bonds tends to be diminished.

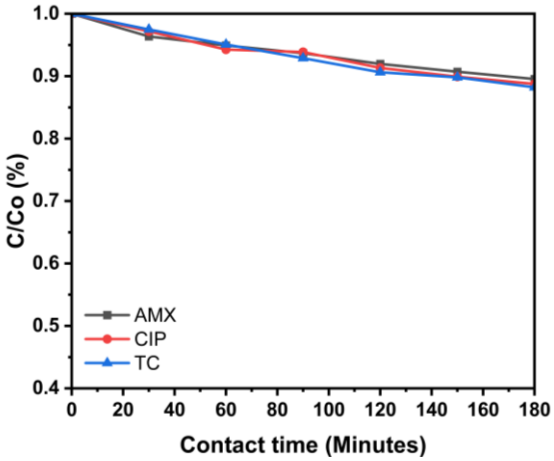

Fig. 9. Decreasing antibiotic concentration on photolysis process

During the process of photolysis, H_2O molecules can be broken apart by absorbing UV irradiation and creating ·OH and h^+ radicals in a water photolysis reaction. The photolysis reaction can be represented by the equation 9-10.

$$H_2O + hv \rightarrow H_2O^* \quad (9)$$

$$H_2O^* + hv \rightarrow \cdot OH + h^+ \quad (10)$$

The production of ·OH radicals in the water photolysis reaction is quite difficult, resulting in the development of only a limited number of ·OH radicals. As a result, the degradation efficiency of antibiotics using only UV tends to be relatively low.

The photocatalyst process is a type of degradation that employs a catalyst and photons. In this investigation, Cu-Bi_2O_3 was used as the catalyst, while UV light was used as the photon source. Fig. 10 depicts the results of degradation with a Cu-Bi_2O_3 catalyst. Each antibiotic demonstrates an independent percentage of degradation efficiency. Tetracycline (TC) had the highest removal efficiency value at 69.46%, which indicates that 69.46% of the TC compound was effectively degraded. The removal efficiency of Ciprofloxacin (CIP)-type antibiotics was 61.72%. The antibiotic type with the lowest removal efficiency is amoxicillin (AMX) at 52.06%.

The photocatalytic process occurs continuously during the process of irradiation. This is an advantage over other processes, such as adsorption and photolysis. Antibiotics will become increasingly degraded as irradiation time increases. This is evidenced by comparing the concentrations of

antibiotics at contact time and their concentrations before degradation, which decreased with the length of irradiation time.

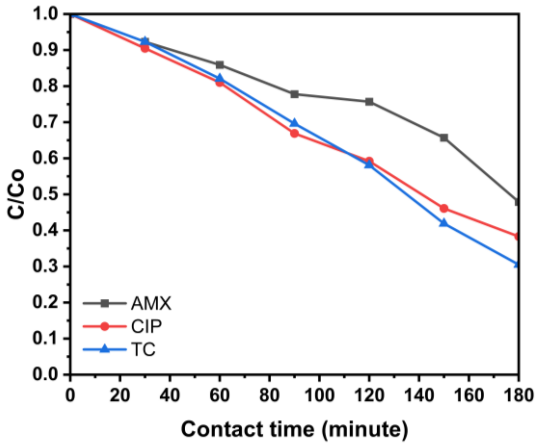

Fig. 10. Antibiotic concentration during photocatalytic process

The efficacy value of Cu-Bi_2O_3 material degradation differed for each antibiotic. This is due to distinctions in the chemical structure of each antibiotic. Each antibiotic possesses unique properties and structures, and consequently responds differently to degradation. The chemical formula for the antibiotic tetracycline is $C_{22}H_{24}N_2O_8$. In this study, Cu-Bi_2O_3 was optimal for degrading TC-type antibiotics, as indicated by the high degradation efficiency values obtained.

A comparative analysis of the efficiency degradation previously documented in the literature for the degradation of AMX, CIP, and TC using photocatalysis revealed that the results obtained in the current study are consistent with those reported by other authors. Zambrano et.al also reported that TC was degraded faster than CIP in the photocatalytic process [53]. However, in degrading AMX-type antibiotics, Cu-Bi_2O_3 has low efficiency. AMX was found to be the most refractory compound among the studied antibiotics. The experimental findings indicate that the structure of the targeted antibiotic also influences the efficiency of the photocatalyst. AMX has a very complex structure, consisting of four basic components: a thiazolidine ring, a beta-lactam ring, a side chain, an amino group. The beta-lactam ring and amino group is a difficult-to-degrade compound structure [54]. Therefore, AMX has the lowest degradation efficiency value in this investigation.

The variation in degradation efficiency values is also impacted by the interplay between Cu metals and antibiotics. The study conducted by Cvijan et al. presents a comprehensive overview of the interactions between Cu^{2+} and different antibiotics. TC is a widely used antibiotic in both human and veterinary medicine. The TC compound consists of five hydroxyl groups, two carbonyl groups, and one urea group. These compounds possess many ionized functional groups and demonstrate a remarkable capacity to bind copper ions. The presence of Cu^{2+} complex ions counteract the antibacterial activity of TC, leading to its effective degradation. According to the findings of this investigation, Poole K discovered that Cu^{2+} ion has a strong affinity for the TC molecule, leading to its effectiveness in degrading antibiotic activity [55].

The photocatalytic process produces superior results compared to adsorption and photolysis. Photocatalysis is preferable to adsorption because the UV-activated Cu-Bi_2O_3 catalyst material produces more radical species. In addition, the Cu-Bi_2O_3 catalyst material does not reach the saturation point during the continuous irradiation procedure, as it did during the adsorption method.

The photocatalytic method is superior to photolysis because the presence of a Cu-Bi_2O_3 catalyst increases the number of radical species that degrade antibiotics. As a consequence, antibiotic degradation occurs more rapidly, resulting in high values of effectiveness. The photolysis method, which employs only ultraviolet light as a photon source, generates fewer radical species because the Cu-Bi_2O_3 catalyst material does not play a role in this process, so electron/hole pairs is not generate.

When ultraviolet light strikes Cu-Bi_2O_3, electrons are excited from the valence band to the conduction band. The excitation caused electron-hole pairs to form in the Cu-Bi_2O_3 semiconductor material. Electrons will initiate reduction reactions, whereas holes will initiate oxidation reactions. Due to the oxidation of (H_2O/·OH) by holes, the reaction in an aqueous solutions result in the formation of hydroxyl radicals The presence of oxygen (O_2) dissolved in water, on the other hand, causes the formation of superoxide radicals owing to the reduction of O_2 by electrons. These radical species oxidize the antibiotic compounds deposited on the surface of Cu-Bi_2O_3 to form simpler compounds that decrease their concentration [56].

3.4. Degradation rate of antibiotics

Fig. 11 shows the relationship between response rate and antibiotic degradation process duration:

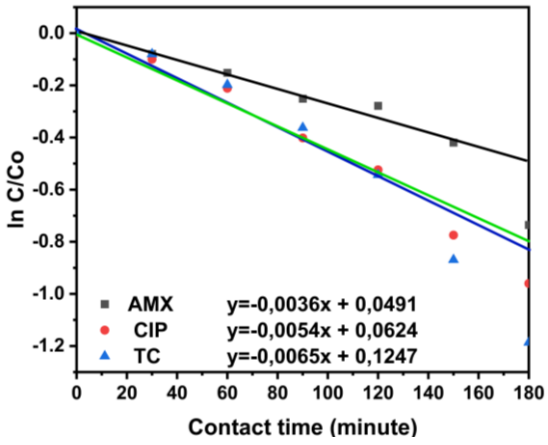

Fig. 11. Antibiotic degradation rate

The results of the reaction rate constants in the AMX, CIP and TC degradation processes were 0.0036 (minutes^{-1}), 0.0054 (minutes^{-1}) and 0.0065 (minutes^{-1}) respectively. The highest reaction rate was obtained in the TC degradation process, while the lowest was in the AMX degradation process. The rate of degradation reaction describes the speed of the material in degrading antibiotics. The higher the value of the reaction rate, the faster the material degrades the antibiotic so that the antibiotic contained decreases. The magnitude of this reaction rate corresponds to the degradation efficiency value of each type of antibiotic that has been described previously.

4. Conclusion

Cu-Bi_2O_3 successfully synthesized using precipitation-

assisted-microwave method at varying concentration of Cu for effective removal of AMX, CIP, and TC antibiotics from water. The test results indicated that the photocatalytic method was more effective than the adsorption and photolysis methods for antibiotic removal. Cu-Bi_2O_3 was more effective at degrading TC-type antibiotics than AMX- and CIP-type antibiotics, with a removal efficiency value 69.46% greater. The study of degradation reaction kinetics revealed that Cu-Bi_2O_3 has a high reaction rate constant of the first order. Cu-Bi_2O_3 has the potential to be utilized in the treatment of pharmaceutical wastewater containing antibiotics due to its high antibiotic removal efficiency and rapid degradation rate.

Acknowledgements

This work was supported by The Ministry of Education, Culture, Research, and Technology of Republic Indonesia by PMDSU Batch VI Scheme with contract no.: 345-41/UN7.D2/PP/IV/2023.

References

1. I. Kurniawan, S. Nasir, Hermansyah, and Mardiyanto, T*he screening of potential antibiotics from hospital wastewater in tropical region (case study at Palembang, South Sumatra, Indonesia),* Pollut. Res. 36 (2017) 343–351.
2. I. Kurniawan, I. Kurniawan, P. Dian, and A. Huda, *The Relationship between the Level of Antibiotic Use in Hospitals and the Potential for Antibiotic Contamination in Public Waters,* (2019) 165–173.
3. A. Shimizu *et al.*, *Ubiquitous occurrence of sulfonamides in tropical Asian waters,* Sci. Total Environ. 452–453 (2013) 108–115.
4. M. Östman, R. H. Lindberg, J. Fick, E. Björn, and M. Tysklind, *Screening of biocides, metals and antibiotics in Swedish sewage sludge and wastewater,* Water Res. 115 (2017) 318–328.
5. J. Fick, H. Söderström, R. H. Lindberg, C. Phan, M. Tysklind, and D. G. J. Larsson, *Contamination of surface, ground, and drinking water from pharmaceutical production,* Environ. Toxicol. Chem. 28 (12)(2009) 2522–2527.
6. T. Yang et al., *Enhanced photocatalytic ozonation degradation of organic pollutants by ZnO modified TiO2 nanocomposites,* Appl. Catal. B Environ. 221 (2018) 223–234.
7. J. Ding, Z. Dai, F. Qin, H. Zhao, S. Zhao, and R. Chen, *Z-scheme BiO1-xBr/Bi2O2CO3photocatalyst with rich oxygen vacancy as electron mediator for highly efficient degradation of antibiotics,* Appl. Catal. B Environ. 205 (2017) 281–291.
8. R. Kafaei et al., *Occurrence, distribution, and potential sources of antibiotics pollution in the water-sediment of the northern coastline of the Persian Gulf, Iran*, Sci. Total Environ.. 627 (2018) 703–712.
9. M. Pan and L. M. Chu, *Occurrence of antibiotics and antibiotic resistance genes in soils from wastewater irrigation areas in the Pearl River Delta region, southern China,* Sci. Total Environ.. 624 (2018) 145–152.
10. T. X. Wang, H. P. Liang, D. A. Anito, X. Ding, and B. H. Han, E*merging applications of porous organic polymers in visible-light photocatalysis,* J. Mater. Chem. A. 8 (2020) 7003–7034.
11. N. Czekalski, T. Berthold, S. Caucci, A. Egli, and H. Bürgmann, *Increased levels of multiresistant bacteria and resistance genes after wastewater treatment and their dissemination into Lake Geneva, Switzerland,* Front. Microbiol. 3 (2012) 1–18.
12. P. Semeraro et al., *Photocatalytic degradation of tetracycline by zno/γ-fe2o3 paramagnetic nanocomposite material,* Nanomaterials 10 (2020) 1–12.
13. G. Li, T. Yan, H. Zhao, and D. Liu, *Effective removal of nitroimidazole antibiotics in aqueous solution by an aluminum-based metal-organic framework: Performance and mechanistic studies,* J. Solid State Chem. 317 (2023) 131932
14. S. Wu, H. Hu, Y. Lin, J. Zhang, and Y. H. Hu, *Visible light photocatalytic degradation of tetracycline over TiO2,* Chemical Engineering Journal 382 (2020).
15. A. Gupta and A. Garg, *Degradation of ciprofloxacin using Fenton's oxidation: Effect of operating parameters, identification of oxidized by-products and toxicity assessment,* Chemosphere 193 (2018) 1181–1188.
16. X. Zhang, W. Guo, H. H. Ngo, H. Wen, N. Li, and W. Wu, *Performance evaluation of powdered activated carbon for removing 28 types of antibiotics from water,* J. Environ. Manage. 172 (2016) 193–200.
17. T. Saitoh, K. Shibata, K. Fujimori, and Y. Ohtani, *Rapid removal of tetracycline antibiotics from water by coagulation-flotation of sodium dodecyl sulfate and poly(allylamine hydrochloride) in the presence of Al(III) ions,* Sep. Purif. Technol. 187 (2017) 76–83.
18. I. Senta, S. Terzic, and M. Ahel, *Occurrence and fate of dissolved and particulate antimicrobials in municipal wastewater treatment,* Water Res. 47 (2012) 705-714.
19. L. Feng, M. E. Casas, L. D. M. Ottosen, H. B. Møller, and K. Bester, *Removal of antibiotics during the anaerobic digestion of pig manure,* Sci. Total Environ. 603 (2017) 219-225.
20. E. Shang, Y. Li, J. Niu, S. Li, G. Zhang, and X. Wang, *Photocatalytic degradation of perfluorooctanoic acid over Pb-BiFeO3/rGO catalyst: Kinetics and mechanism,* Chemosphere 211 (2018) 34-43.
21. Y. Yang et al., R*ecent advances in application of graphitic carbon nitride-based catalysts for degrading organic contaminants in water through advanced oxidation processes beyond photocatalysis: A critical review,* Water Research 184 (2020).
22. Y. M. Hunge, A. A. Yadav, S.-W. Kang, and H. Kim, *Photocatalytic degradation of tetracycline antibiotics using hydrothermally synthesized two-dimensional molybdenum disulfide/titanium dioxide composites,* J. Colloid Interface Sci. 606 (2022) 454-463.
23. S. Li, Z. Wang, X. Zhao, X. Yang, G. Liang, and X. Xie, *Insight into enhanced carbamazepine photodegradation over biochar-based magnetic photocatalyst Fe3O4/BiOBr/BC under visible LED light irradiation,* Chemical Engineering Journal 360 (2019) 600-611.
24. E. Márquez Brazón, C. Piccirillo, I. S. Moreira, and P. M. L. Castro, *Photodegradation of pharmaceutical persistent pollutants using hydroxyapatite-based materials,* Journal of Environmental Management 182 (2016) 486-495.
25. J. Wang and R. Zhuan, *Degradation of antibiotics by advanced oxidation processes: An overview,* Sci. Total Environ. 701 (2020) 1350123.
26. F. Sa'adah, H. Sutanto, and Hadiyanto, *Optimization of the Bi2O3/Cu synthesis process using response surface methodology as a tetracycline photodegradation agent*, Results In Engineering 16 (2022) 100521.
27. X. Bai, W. Chen, B. Wang, T. Sun, B. Wu, and Y. Wang, *Photocatalytic Degradation of Some Typical Antibiotics: Recent Advances and Future Outlooks,* Int. J. Mol. Sci. 23 (2022).
28. V. Thakur et al., *Photocatalytic behaviors of bismuth-based mixed oxides: Types, fabrication techniques and mineralization mechanism of antibiotics,* Chem. Eng. J. 475 (2023) 146100.
29. P. L. Koo, Z. Y. Choong, C. He, Y. Bao, N. F. Jaafar, and W. Da Oh, *Effect of metal doping (Me = Zn, Cu, Co, Mn) on the performance of bismuth ferrite as peroxymonosulfate activator for ciprofloxacin removal,* Chemosphere 318 (2023) 137915.

30. B. A. Utami, H. Sutanto, I. Alkian, F. Sa'Adah, and E. Hidayanto, *Efficient degradation of amoxicillin using Bi2O3/Fe synthesized by microwave-assisted precipitation method,* Cogent Eng. 9 (2022).
31. S. Singh and R. Sharma, *Bi2O3/Ni-Bi2O3 system obtained via Ni-doping for enhanced PEC and photocatalytic activity supported by DFT and experimental study,* Sol. Energy Mater. Sol. Cells 186 (2018) 208-216.
32. G. Viruthagiri, P. Kannan, and N. Shanmugam, *Photocatalytic rendition of Zn2+-doped Bi2O3 nanoparticles,* Photonics Nanostructures - Fundam. Appl. 32 (2018) 35-41.
33. W. Zhang, S. Gao, and D. Chen, Prepa*ration of Ce3+ doped Bi2O3 hollow needle-shape with enhanced visible-light photocatalytic activity,* J. Rare Earths 37 (2019) 726-731.
34. J. Wang et al., *One-step fabrication of Cu-doped Bi2MoO6 microflower for enhancing performance in photocatalytic nitrogen fixation,* J. Colloid Interface Sci. 638 (2023) 427-438.
35. M. Matouq, T. Tagawa, and N. Susumu, *High frequency ultrasound waves for degradation of amoxicillin in the presence of hydrogen peroxides for industrial pharmaceutical wastewater treatment,* Glob. Nest J. 16 (2014) 805-813.
36. M. Hassan et al., *Effect of the C/N ratio on biodegradation of ciprofloxacin and denitrification from low C/N wastewater as assessed by a novel 3D-BER system*, Sustainable 12 (2020) 1-19.
37. P. Zhang, Y. Li, Y. Cao, and L. Han, Ch*aracteristics of tetracycline adsorption by cow manure biochar prepared at different pyrolysis temperatures,* Bioresour. Technol. 285 (2019) 121348.
38. F. Riyanti, H. Hasanudin, A. Rachmat, W. Purwaningrum, and P. L. Hariani, *Photocatalytic degradation of methylene blue and Congo red dyes from aqueous solutions by bentonite-Fe3O4 magnetic,* Commun. Sci. Technology 8 (2023) 1-9.
39. W. Qin, J. Qi, and X. Wu, *Photocatalytic property of Cu2+-doped Bi2O3 films under visible light prepared by the sol–gel method*, Vacuum 107 (2014) 204-207.
40. V. Dutta et al., *Recent progress on bismuth-based Z-scheme semiconductor photocatalysts for energy and environmental applications,* Journal of Environmental Chemical Engineering 8 (2020).
41. I. Manouchehri, D. Mehrparvar, R. Moradian, K. Gholami, and T. Osati, *Investigation of structural and optical properties of copper doped NiO thin films deposited by RF magnetron reactive sputtering,* Optik 127 (2016) 8124-8129.
42. S. Mani Menaka, G. Umadevi, and M. Manickam, *Effect of copper concentration on the physical properties of copper doped NiO thin films deposited by spray pyrolysis,* Mater. Chem. Phys. 191 (2017) 181-187.
43. S. Labib, Prepa*ration, characterization and photocatalytic properties of doped and undoped Bi2O3 Preparation, characterization and photocatalytic properties of doped and undoped Bi2O3*, J. Saudi Chem. Soc. 21 (2017) 664-672.
44. X. Wang et al., T*he influence of crystallite size and crystallinity of anatase nanoparticles on the photo-degradation of phenol,* J. Catalysis 310 (2014) 100-108.
45. M. Sarani et al., *Green synthesis of Ag and Cu-doped Bismuth oxide nanoparticles: Revealing synergistic antimicrobial and selective cytotoxic potentials for biomedical advancements, J*. Trace Elem. Med. Biol. 81 (2023) 127325.
46. R. T. Nuaman and Huda Saadi Ali, S*tudy of the structural and optical properties of Bi2O3:Cu Thin FIlms as a Function of Different Doped Ratios,* Math. Statictician Eng. Appl. 71 (2022) 1306-1315.
47. A. Sharma, A. Mittal, S. Sharma, K. Kumari, S. Maken, and N. Kumar, *Cu2+-doped α–β phase heterojunctions in Bi2O3 nanoparticles for enhanced photocatalytic degradation of organic dye rhodamine B,* Appl. Nanoscience 12 (2022) 151-164.
48. A. Sharma, M. Varshney, H. J. Shin, B. H. Lee, K. H. Chae, and S. O. Won, *Effect of Cu insertion on structural, local electronic/atomic structure and photocatalyst properties of TiO2, ZnO and Ni(OH)2 nanostructures*, Mater. Chem. Phys.191 (2017) 129-144.
49. M. T. M. H. Hamad and M. E. El-Sesy, *Adsorptive removal of levofloxacin and antibiotic resistance genes from hospital wastewater by nano-zero-valent iron and nano-copper using kinetic studies and response surface methodology*, Bioresour. Bioprocess 10 (2023) 1-29.
50. D. Weerakoon et al., *A critical review on current urea removal technologies from water: An approach for pollution prevention and resource recovery,* Sep. Purif. Technol. 314 (2023) 123652.
51. X. Zhang, T. Bhattacharya, C. Wang, A. Kumar, and P. V. Nidheesh, *Straw-derived biochar for the removal of antibiotics from water: Adsorption and degradation mechanisms, recent advancements and challenges*, Environmental Research 237 (2023) 116998.
52 R. Delli Compagni et al., *Modeling tools for risk management in reclaimed wastewater reuse systems: Focus on contaminants of emerging concern (CECs),* in Advances in Chemical Pollution, Environmental Management and Protection 6 (2020) 181-220.
53. J. Zambrano, P. A. García-Encina, J. J. Jiménez, R. López-Serna, and R. Irusta-Mata, P*hotolytic and photocatalytic removal of a mixture of four veterinary antibiotics,* J. Water Process Eng. 48 (2022).
54. I. Anastopoulos et al., *Removal of caffeine, nicotine and amoxicillin from (waste)waters by various adsorbents. A review*, Journal of Environmental Management 261 (2020).
55. K. Poole, *At the Nexus of Antibiotics and Metals: The Impact of Cu and Zn on Antibiotic Activity and Resistance*, Trends Microbiol. 25 (2017) 820-823.
56. Y. Qu, X. Xu, R. Huang, W. Qi, R. Su, and Z. He, *Enhanced photocatalytic degradation of antibiotics in water over functionalized N,S-doped carbon quantum dots embedded ZnO nanoflowers under sunlight irradiation*, Chemical Engineering Journal 382 (2020).